Journal of Electron Devices, Vol. 4, 2006, pp. 89-92

© JED [ISSN: 1682 -3427]

Journal of Electron Devices

Experimental investigations of an internal flow generated by porous injection

C. Fournier[(1)]*, F. Bataille[(2)] and M. Michard[(1)]
(1) Centre de Thermique de Lyon, UMR CNRS 5008, INSA de Lyon, Bat Sadi Carnot, 20 av. Albert Einstein, 69621 Villeurbanne Cedex, France
(2) PROMES, UPR CNRS 8521, Rambla de la thermodynamique, Tecnosud, 66100 Perpignan, France
*Correspondence author: Fax: +01 04 72 43 70 77 Email: clarisse.fournier@insa-lyon.fr

ABSTRACT

A non-isothermal channel flow generated by a porous wall has been investigated experimentally. Mean flow properties and statistics are obtained by analysing instantaneous measurements of the velocity field (2D Particle Image Velocimetry) and the temperature field (cold wire thermometer). The choice of a porous material which generates pseudoturbulence has permitted to obtain a turbulent flow. Experimental data are compared with computational results including axial mean velocity profiles and turbulent stresses and a good agreement is obtained for these quantities.

Keywords: blowing, turbulent channel flow, heat transfer, Particle Image Velocimetry, cold wire thermometer

INTRODUCTION

Flows induced only by blowing through permeable walls have been the subject of many isothermal studies due to their importance in various engineering applications. These include for examples flow filtration process [1] or diffuse separation of gaseous isotopes [2]. There are many geometries found in the literature which model the combustion in solid propellant rocket motors with a porous wall through which fluid is normally injected [3,4]. This type of channel flow presents some characteristics quite different from that observed in a pipe or in a boundary layer flow with impermeable walls. The parietal injection involves in particular the curve of the streamlines. It is also an accelerated flow which evolves significantly according to the distance from the center of the channel [5,6]. Analytical solutions of the laminar, steady, incompressible and two-dimensional channel flow generated by a parietal injection have been investigated by several authors [1-3]. These solutions are rather close to numerical and experimental results before a critical turbulence threshold implies a transition process of the mean axial velocity. The transition behavior of the velocity field has been numerically investigated by several authors [5-11].

In this paper, we present experiments realized in an anisothermal channel with a porous wall. The experimental set-up permits to investigate the behavior of mean and fluctuating fields of velocity and temperature and to compare results with computations based on RANS simulations.

EXPERIMENTAL FACILITIES

Test channel

The main components of the experimental apparatus are schematically shown in figure 1. A more complete description of the experimental set-up is available in [12]. Ambient air is injected into the channel through a $495 \times 200 \times 3\ mm^3$ porous plate, made of sintered-stainless-steel, 30 % porosity and 30 μm average pore diameter. A 150 mm box fitted under the porous plate is designed to deliver an uniform injection through it. The channel is limited on its two lateral sides by windows in order to permit optical measurements and the roof of the test section consists of an heated stainless steel foil (50 μm thickness). The channel height e is equal to 10 mm giving a lenght to height ratio of 50. The main control parameter of the dynamic flow is a transverse Reynolds number, Re_{in} based on the injection velocity V_{in} and the height e of the channel ; experiments conducted for $94 < Re_{in} < 220$ are presented in this paper. The order of magnitude of the mean temperature difference between the upper wall and the injected air is 45 $°C$.

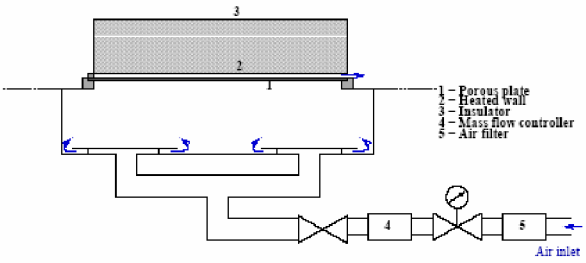

Figure 1
Experimental set-up

Techniques measurements

The instantaneous velocity fields are measured in the $(x-y)$ plane at different downstream locations and for different

Re_{in} with a bidimensional Particle Image Velocimetry (*Cf.* figure 2). The main characteristics of the system used are:

- The seeding particles are micron-sized oil dropplets.
- The acquisition rate is equal to 10 Hz.
- 500 instantaneous fields are used to calculate the mean velocity profiles and statistics.
- The size of the smallest interrogation area are 32×32 pixels which corresponds approximately to 55 μm.

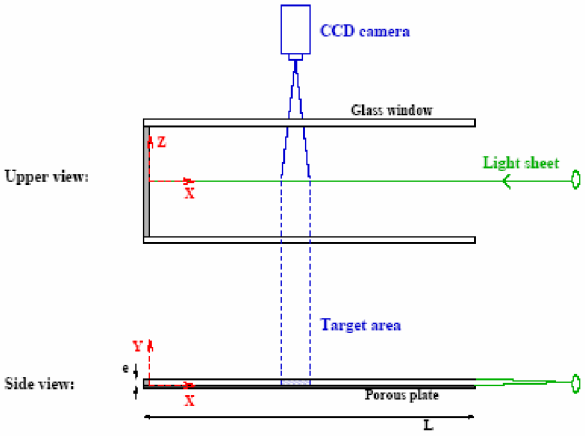

Figure 2
Principle of PIV measurement

The instantaneous temperature is measured by a cold platinium wire thermometer with a diameter equal to 1 μm. The probe resistance is about 49 Ω and the current intensity through the wire is near 0.1 mA. In the range of temperature used, the response of the wire is a linear function of fluid temperature. Different measurements made near the head end of the channel have been realized.

RESULTS

Instantaneous velocity field

Characteristic instantaneous velocity field captured in the $(x - y)$ plane is presented in figure 3. A large turbulence level is observed and this phenomenon can be explained by the porous material characteristics. A microscopic observation of a sintered stainless steel material reveals highly random pore configuration which produces spatial velocity variations (called pseudoturbulence). Previous studies [13, 14] showed that the flow through this type of porous medium seemed to coalesce into large scale jets which affect the flow behavior.

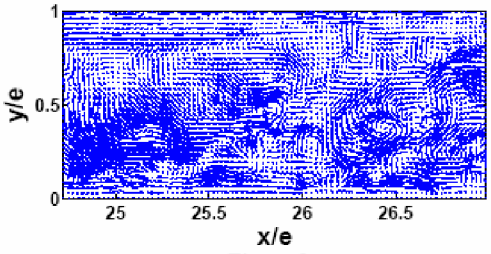

Figure 3
Instantaneous velocity field for $Re_{in} = 189$.

Velocity profiles

Figure 4 and 5 show mean streamwise velocity profile and RMS velocity normalized by the bulk velocity at $x/e = 41$ and for $Re_{in} = 94$. A comparison with simulations based on a Reynolds Stress Model is presented. Details about the numerical approach and the model of turbulence used are presented in the following reference [11]. In most cases, it is difficult to simulate the geometric details of the porous material surface. Therefore, the porous wall is often replaced by an equivalent material through which the flow is injected with uniform properties (velocity, temperature,...). For the numerical results presented in this paper, the injection is modelled by using additional sources at the porous wall in the resolved equations. A constant source of normal velocity fluctuations characterized by a dimensionless coefficient $\sigma = \sqrt{\frac{\overline{vv}}{V_{in}}} = 0.2$ which traduces the level of normal velocity fluctuations at the exit of the porous surface is added.

In this section of the channel, we observe that the velocity profile tends to a symetrical profile which is more characteristic of a developed channel flow bounded by impermeable walls. The results obtained for various Reynolds numbers (not presented in this paper) confirm these results and show that the maximum velocity still approaches the higher wall when the Reynolds number of injection increases.

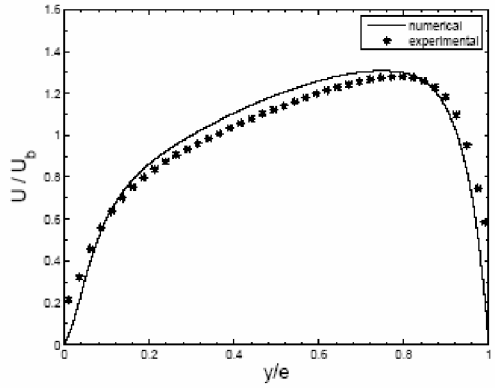

Figure 4
Mean velocity profiles for $Re_{in} = 94$ and $x/e = 41$

The development of turbulence (figure 5) occurs at two locations, near the impermeable and the porous walls. The turbulent profile obtained with numerical simulation is very near the experimental one. The general shape and the level of the RMS profiles are especially well reproduced with numerical model.

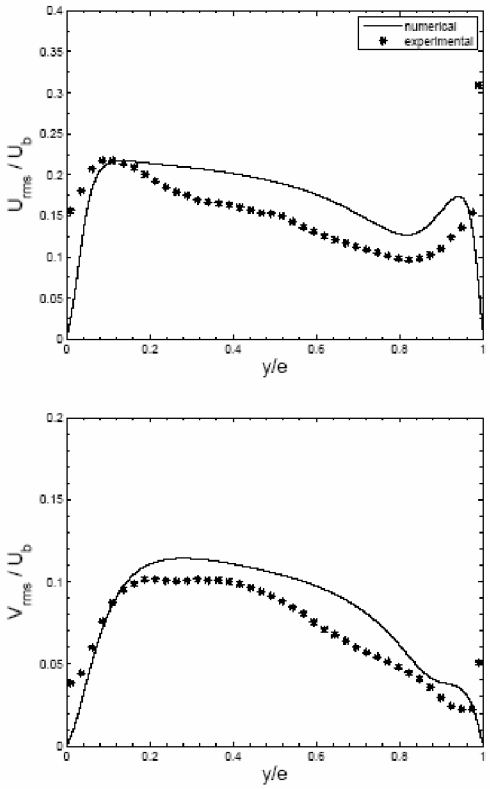

Figure 5
RMS velocity profiles for $Re_{in} = 94$ and $x/e = 41$

Temperature profiles

Figure 6 and 7 present mean and RMS temperature profiles at $x/e = 41$ for different Reynolds number between 94 and 220. In order to compare the various cases, it is necessary to present results normalized by the temperature difference imposed between the two walls. The evaluation of the injected temperature was carried out by extrapolation of the temperature profiles. As the temperature variation is almost null close to the porous wall, this estimate seems correct. Moreover the confrontation of this value with that obtained thanks to a thermocouple positioned in the injected box is conclusive. The same method was applied for the temperature of the higher wall. In this case, one probably slightly underestimates the temperature variation and thus the wall temperature.

In all cases, the lower part of the channel (including between $y/e = 0$ and $y/e = 0.5$) is characterized by an uniform mean temperature, very near to the temperature of the air injected. When the Reynolds number of injection increases, this zone extends; in other words, the thickness of thermal boundary layer decreases with the increase of Re_{in}. We noticed a peak of fluctuations near the higher wall. Apart from this peak, the levels of temperature fluctuations are very low and represent the noise levels of measurement. All the curves present a peak of fluctuations of similar intensity. Only the width of the peak decreases with the increase in the Reynolds number of injection.

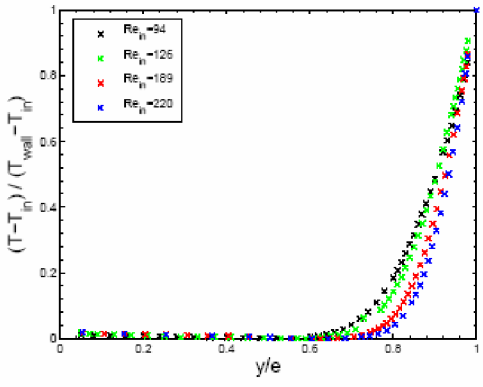

Figure 6
Mean temperature profiles at $x/e = 41$ for different Re_{in}

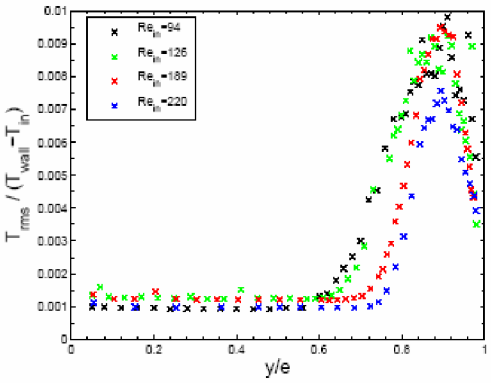

Figure 7
RMS temperature profiles at $x/e = 41$ for different Re_{in}

In order to complete these results, we present on figure 8 and 9 an assessment of the spectral densities of temperature at $x/e = 41$ for two different Re_{in}. Three positions defined by $y/e = 0.8$, 0.9 and 0.965, being in the thermal boundary layer, were represented. Spectral densities were normalized by the variance of the temperature fluctuations in order to be able to compare the various series of measurements characterized by different variations in tem-

perature from one wall with the other. The spectral densities traced in the thermal boundary layer are rather similar: we observe a plate in the very low frequencies and a cut-off frequency which decreases with the Reynolds number of injection. The behavior of the spectral densities when the frequency increases shows a rather fast decrease of the spectral densities, on which are superimposed amplified frequency bands.

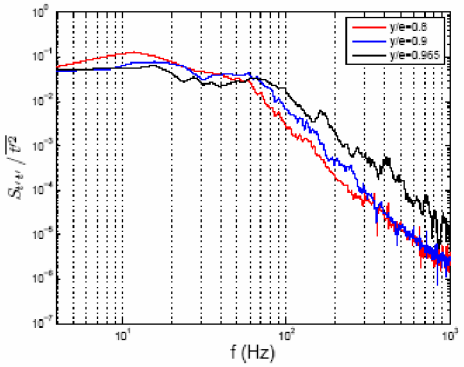

Figure 8
Spectral densities of temperature for $Re_{in} = 94$

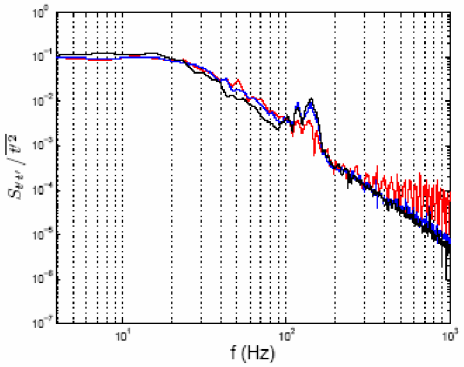

Figure 9
Spectral densities of temperature for $Re_{in} = 220$

CONCLUSIONS

The experimental set-up of an anisothermal channel flow generated by a porous injection with high-level of pseudo-turbulence permits to observe a turbulent flow development. The effect of the injection Reynolds number on velocity and temperature profiles has been studied.

The comparison of the aerodynamic and thermal fields obtained with two types of porous materials, being characterized by their porous matrix and by the pore size will permit to highlight the impact of the microstructure of porous material on the flow development.

References

[1] G.I. Taylor "Fluid Flow in Regions Bounded by Porous Surfaces, Proceedings of the Royal Society of London", Series 234A, **1199**, pp. 456-475 (1956).

[2] A. Berman "Laminar Flow in Channels with Porous Walls", Journal of Applied Physics, **24**(9) (1953).

[3] F.E.C. Culick "Rotational Axisymmetric Mean Flow and Damping of Acoustic Waves in Solid Propellant Rocket Motors", AIAA Journal, **4**(8), pp. 1462-1464 (1966).

[4] R. Dunlap, P.G. Willoughby and R.W. Hermsen "Flowfield in the Combustion of a Solid Propellant Rocket Motor", AIAA Journal, **12**(12), pp. 1440-1442 (1974).

[5] R.A. Beddini "Injection-induced Flows in Porous-walled Ducts", AIAA Journal, **24**(11), pp. 1766-1773 (1986).

[6] C. Fournier, F. Bataille and M. Michard, "Transition Characteristics of Flowfield in a non-isothermal Duct with Wall Injection", Proceedings of 4^{th} International Conference on Computational Heat and Mass Transfer, R. Bennacer et al., eds., Tec & Doc, Paris, **2**, pp. 899-904 (2005).

[7] J.C. Traineau, P. Hervat and P. Kuentzmann "Cold-flow Simulation of a two-dimensional Nozzleless Solid-rocket Motor", AIAA Paper 1986-1447 (1986).

[8] T.M. Liou, W.Y. Lien and P.W. Hwang "Transition Characteristics of Flowfield in a Simulated Solid-rocket Motor", J. Propulsion Power, **14**(3), pp. 282-289 (1998).

[9] B. Chaouat "Numerical Predictions of Channel Flows with Fluid Injection using Reynolds-Stress Model", J. Propulsion Power, **18**(2), pp. 295-303 (2002).

[10] S. Apte and V. Yang "Large Eddy Simulation of Internal Flowfield in Porous Chamber with Surface Mass Injection", AIAA Paper 2000-0709 (2000).

[11] C. Fournier, M. Michard and F. Bataille "Numerical Simulations of a Confined Channel Flow driven by non Isothermal Wall Injection", Progress in Computational Fluid Dynamics, vol. 6 (1-3), pp. 129-136 (2006)

[12] C. Fournier "Study of Heat and Mass Transfer in a Channel Flow Generated by Blowing through a Porous Wall", Ph.D. thesis, National Institut of Applied Sciences, France, (2005).

[13] Y.P. Yeh "Injection-induced Flow from Porous Medium in cold-flow Simulation of Solid Rocket Motors" ASME/SAE/ASEE 30^{th} Joint Propulsion Conference and Exhibit, pp. 1-10 (1994)

[14] N. Ramachandran, J. Heaman and A. Smith "An Experimental Study of the Fluid Mechanics associated with Porous Walls" 30^{th} Aerospace Sciences Meeting and Exhibit (1992)